4th Adams Rail Users Conference
Utrecht 28th - 29th April 1999

DYNAMIC SIMULATION OF A FRICTION DAMPED RAILWAY VEHICLE

A.Gugliotta, A.Somà, S. R. Di Mauro

Departement of Mechanical Engineering,

Politecnico di Torino

Keywords: friction dampers, railway, vehicles dynamics

Abstract:
The aim of this work is to study the tangent track lateral stability and curve negotiability of a railway vehicle using friction. The dynamics are investigated by means of numerical simulations of a vehicle modeled using the railway oriented code of ADAMS. Results are presented in comparison to the numerical performances of a currently featured vehicle using hydraulic yaw-dampers.
The analysis of the present-day knowledge of friction has shown that only qualitative predictions can be made about this class of phenomena and consequently the most viable way is the phenomenological approach. As a consequence models of friction dampers of different levels of complexity are proposed.
In a second time these models are implemented on the vehicle model. Due to the large nonlinearites introduced in the system by the friction yaw-dampers, the dynamic behavior of the vehicle is studied resorting to transient analyses. Stability is tested against a lateral impulsive force acting on a wheelset. The effects produced by the variation of the force magnitude are observed and reported. Analyses are carried out in order to show the sensitivity of the critical speed with respect the equivalent conicity angle, the normal load acting between the rubbing surfaces and the ratio between the static and kinetic coefficient of friction.

I. Modeling of friction damper

I.1 Classic Laws of Friction

It is common to assess that friction forces develop when two contacting bodies are pressed against each other and then subject to forces that tend to produce relative sliding. In the following only the resultant of the stresses applied on the surfaces will be considered: the normal load N and the friction force F. [1] .
The friction force is proportional to the normal force:

$$F = \mu_k N \qquad (1)$$

the coefficient of proportionality μ_k is usually refereed to as kinetic coefficient of

friction. The properties featured as Classical Laws of Friction can be summarized in a friction coefficient μ vs. relative velocity (Vr) plot, as follows.

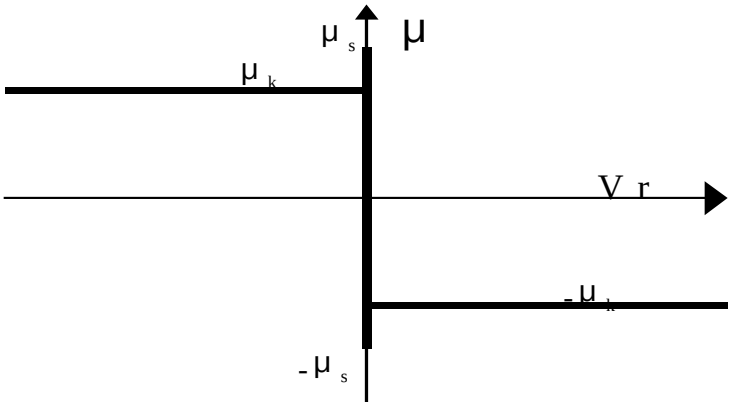

Figure 1: Classic Discontinouous Friction vs. Relative velocity plot

At the onset of sliding the friction coefficient is somehow greater than the kinetic coefficient of friction. In this case, equation III.1 is still valid provided that μ_k is substituted for μ_s. Usually μ_s is quoted as static coefficient of friction. The large majority of friction-damper models start from this curve.

I.2 Comparison of viscous and friction energy loss

It is worthwhile to focus on some aspects concerning the differences between friction dampers and viscous dampers in removing energy from a system.

Assume, conventionally a friction model such that pictured in (piece-wise constant force). If the kinetic friction force is $f_f = \mu_k \cdot N$ (where N is the normal load), and the amplitude of the oscillation is a (thus the stroke of the damper is $2 \cdot a$), the energy dissipated in a complete cycle is

$$E_f = 4 \cdot f \cdot a = 4\mu_k \cdot N \cdot a \qquad (2)$$

In case of a viscous damper assuming a relative sinusoidal motion of the damper ends with frequency λ: $x = a \sin(\lambda \cdot t)$ the relative velocity will be $x' = a\lambda \cos(\lambda \cdot t)$. The damper force is given by $f_d = -c\,x'$, where c is the damping coefficient. Therefore the energy lost in a cycle is:

$$E_d = \int_0^T cx' \cdot x' dt = \int_0^T c \cdot a^2 \cdot \lambda^2 \cdot \cos^2 \lambda t dt =$$

$$= c \cdot a^2 \cdot \lambda^2 \cdot \frac{T}{2} = c \cdot a^2 \cdot \lambda^2 \cdot \frac{\pi}{\lambda} = c \cdot a^2 \cdot \lambda \cdot \pi \qquad (3)$$

Where the period $T = 2 \cdot \pi / \lambda$.

Comparing formula (2) and (3) it is remarkable that the energy lost in a cycle increases with the amplitude of the oscillation in the case of the friction damper, but with the square

of the amplitude of the oscillation in the case of the viscous damper. As it can e seen in *Figure 2* for a certain amplitude the energy lost is equal. For smaller values the energy dissipated by the friction damper is higher, while for bigger values the viscous dampers are more effective. As a consequence friction dampers are expected to be more efficient for small amplitude oscillations, while viscous dampers perform better for higher amplitudes.
On the base of this theoretical observation, experimental results may be interpreted. For subcritical speed, as the amplitude of the oscillations gets always smaller, the friction dampers are more effective than the viscous ones their efficiency becoming more relevant for smaller amplitude oscillations. Thus friction dampers are expected to extinguish oscillations more quickly. For supercritical speed the oscillations amplify and thus viscous dampers are more efficient.

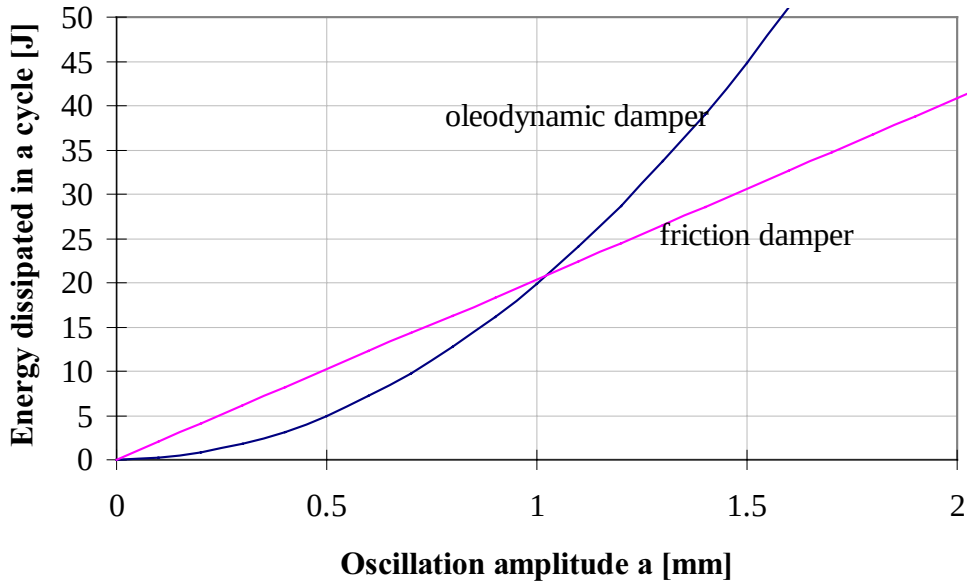

Figure 2: Energy lost per cycle for friction and oleodynamic dampers. (c=202 N·s/mm; λ=5 Hz; □=0.15; N=34000 N)

I.3 Friction basic step function model

In friction damper modelling the first problem encountered is that the friction force (or equivalently the dimensionless ratio μ) is not a unique function of the relative velocity. It depends on the sign of the relative velocity when this is different from zero and can assume any value in the range $[-\mu_s, \mu_s]$ when the relative velocity vanishes, in order to keep the contacting surfaces from sliding. An exact depiction of this behavior would require a change in the equations of motion when the velocity passes through the origin. This approach is usually known as *halting method*, as the time integration algorithm is to be halted, equation of motion changed and simulation continued each time the relative velocity vanishes. The main advantage of the halting methods is that the theoretical law of friction pictured in Figure 1 is followed precisely.
The other approach found in literature consists in smoothing the discontinuous law of friction obtaining a curve having a greater order of continuity. The classical friction properties are not respected, but the modeling become much easier as general purpose

software can be used. If the static coefficient of friction is neglected a smooth friction model can be easily obtained in ADAMS using the step function with the following syntax:

$$\mu = \text{STEP}\ (\ Vr, -\varepsilon,\ \mu_k\ , \varepsilon, -\mu_k\ )$$

which corresponds to the following function:

$$\mu = \begin{cases} +\mu_k \Leftrightarrow Vr < -\varepsilon \\ -\mu_k \Leftrightarrow Vr > \varepsilon \\ \mu_k - \mu_k \left(\dfrac{Vr - \mu_k}{\varepsilon} \right)^2 \left[3 - 2 \left(\dfrac{Vr - \mu_k}{\varepsilon} \right) \right] \Leftrightarrow -\varepsilon \le Vr \le \varepsilon \end{cases}$$

I.2 Static-Kinetic Friction Damper Model

A more complete model for a friction damper takes into account the possibility of stiction. Due to this behavior, it becomes unfeasible to retain the relative velocity as the unique variable.

It is common experience confirmed by numerous experimental results that the increase of the friction force occurs only at onset of motion, i.e. when the velocity is zero and its absolute value is increasing. While, when the relative velocity is reaching zero from a nonzero value no significant variations are observed in the coefficient of friction. The rest is the necessary condition for the friction coefficient to be allowed to increase, the restart requires its drop.

The behavior of the coefficient of friction about the vanishing velocities has been studied in many works meant to formulate phenomenological laws of friction . In the majority of cases ([1], [2], [3], [4], [5])characteristics such that pictured in Figure 3 have been observed.

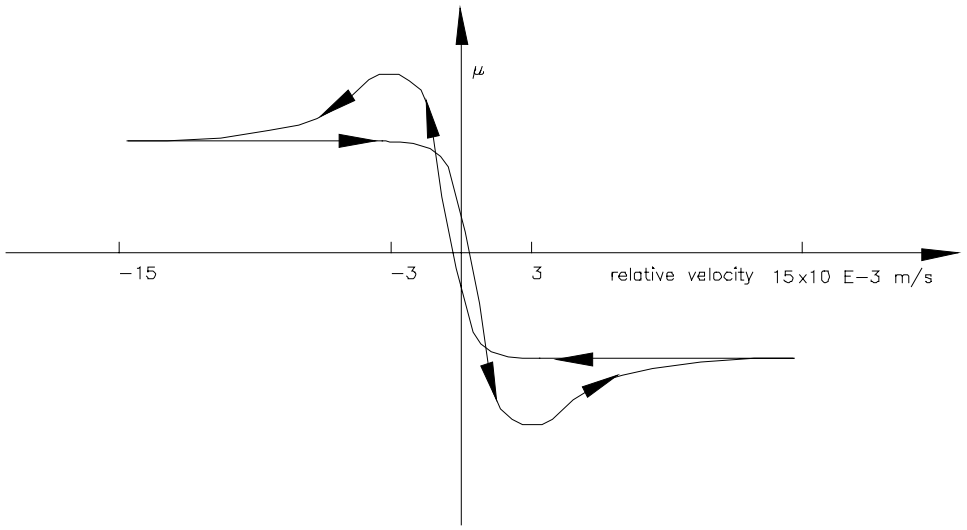

Figure 3: Behavior of the coefficient of friction about the origin. Qualitative plot reproducing only the order of magnitude of cited experimental results

From the figure 3 it is apparent that:

i. The coefficient of friction does not change abruptly, but continuously with the relative velocity if the resolution is of the order of 1 mm/s or smaller.

ii. The coefficient of friction cannot pictured as a unique function of the relative velocity.

The first point makes it clear that the discontinuous law reported in Figure 1, apparently not realistic, can be improved in many instances at low cost. The condition for this to happen is that, for the particular application under study, the range within which the coefficient of friction does change is large enough to allow the building of a model able to follow these variations closely, without largely affecting the computation time. As the range of variation of the coefficient of friction is usually reported to be as large as some 10^{-3} m/s , the above condition is likely to be satisfied in many instances.

According to the second point at least another independent variable must be introduced to allow a correct modeling. Neglecting for the moment the hysteresis about the origin it seems reasonable from Figure 3 to consider the relative acceleration.

Introducing directly a two variable function for the coefficient of friction the so obtained damper characteristic is pictured in Figure 4 is obtained.

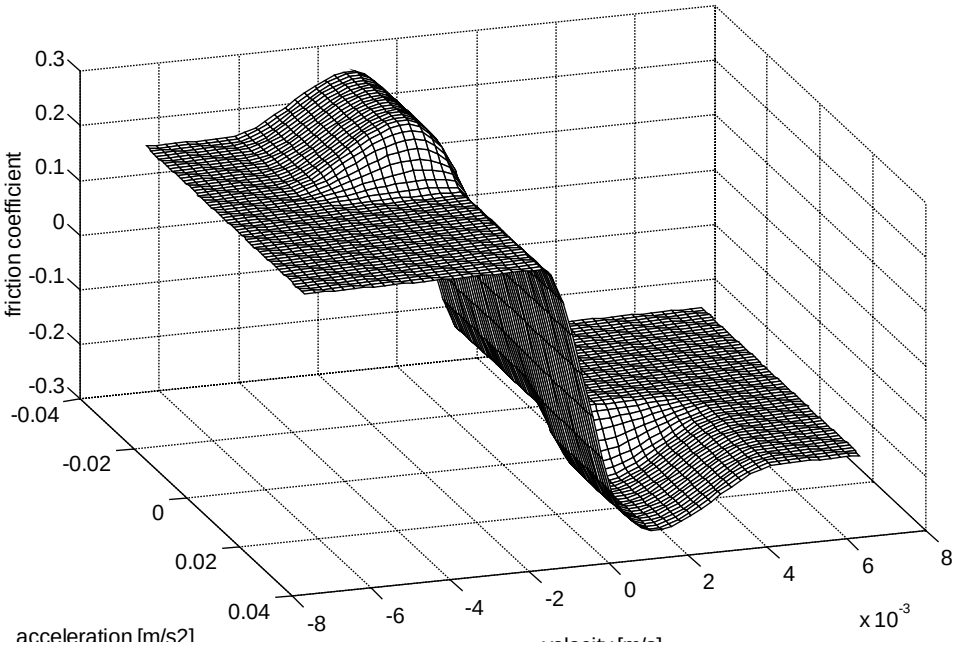

Figure 4: Friction force vs. Relative velocity and acceleration

The robustness of this model is given by the gradual change in the function when the relative acceleration changes its sign. If the dynamics determine a change of the acceleration sign within the range of variation of the coefficient of friction no discontinuity is produced and the simulation can continue. The model of figure 4 has been obtained just utilizing STEP functions.

The expression utilized for generating Figure 4 is:

$$\mu = STEP(Vr,-VK,\mu_k,VK,-\mu_k) +$$
$$-(\mu_s-\mu_k)\cdot[STEP(Vr,0,0,VM,1)-STEP(Vr,VM,0,VD,1)]\cdot$$
$$\cdot STEP(Ar,-AC,0,AC,1)+$$
$$+(\mu_s-\mu_k)\cdot[STEP(Vr,-VD,0,VM,1)-STEP(Vr,VM,0,0,1)]\cdot$$
$$\cdot STEP(Ar,-AC,1,AC,0).$$

Where:

Vr is the relative velocity of the contacting surfaces (1st independent variable)

Ar is the relative acceleration of the contacting surfaces (2nd independent variable)

VD=0.007 m/s is the relative velocity magnitude above which the coefficient of friction becomes definitively constant. Therefore it represents half the amplitude of the range within which variations of the coefficient of friction are considered.

VM=0.003 m/s is the relative velocity magnitude at which the maximum coefficient of friction is to be placed (coefficient of static friction).

VK=0.001 m/s is the relative velocity magnitude at which the friction coefficient raises to its kinetic value if relative velocity and acceleration have opposite signs.

AC=0.005 m/s² is a parameter representing half the amplitude within which the acceleration is subject to modify the shape of the curve. In other words the range [-AC, AC] is that within which the skipping from the outer to the inner curve reported in figure 18 occurs and vice versa.

I.3 Friction model vith series stiffness

Experiments conducted by Wang [2] have shown a plot for the coefficient of friction versus relative velocity having a hysteresis loop near the origin. This behavior has been explained by McMillan [7] as the influence of the stiffness of the bonds between contacting surfaces. The surfaces are supposed to move small distances relative to each other without disrupting the temporary bonds between them and thus the force exerted under this condition is essentially elastic.

These observations show that in many instances a model dynamically more complete, able to account for hysteresis loops observed experimentally, can be obtained including a series stiffness to the rubbing contact of the friction damper. In this case, the force exerted by the damper can be computed resorting to the relevant differential equations.

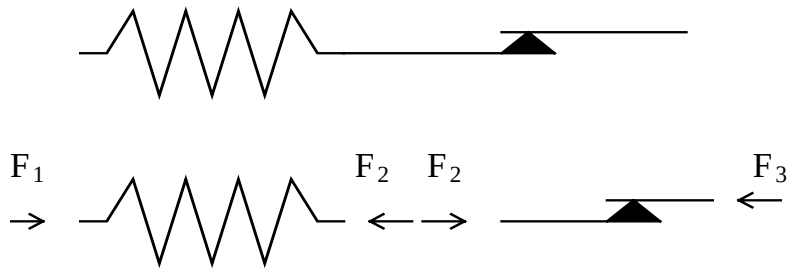

Figure 5 Model of a friction damper with series stiffness

$$\begin{cases} F_1 = F_2 = F_3 = F \\ F_1 = k(x_2 - x_1) \\ F_2 = -\mu(x_3' - x_2', x_3'' - x_2'') \cdot N \end{cases}$$

whence:

$$\begin{cases} k(x_2 - x_1) + \mu(x_3' - x_2', x_3'' - x_2'') \cdot N = 0 \\ F = k(x_2 - x_1) \end{cases}$$

and finally

$$\begin{cases} k(x - x_1) + \mu(x_3' - v, x_3'' - v') \cdot N = 0 \\ x' = v \\ F = k(x_2 - x_1) \end{cases}$$

were we put $x_2 = x$ as x_2 is the new variable introduced by these equations. The stiffness k of the spring will constitute another variable to be identified from experimental results.

II. Simulation of a railway vehicle comparison of performance between viscous and friction antiyaw dampers.

In the following sections the results of the analyses performed on the ADAMS/Rail models of a high-speed passenger vehicle. The ETR 460-BAC and of the ETR 460-FD models are presented.
The ETR 460-BAC is the currently produced vehicle featuring viscous yaw-dampers. The ETR 460-FD is a vehicle model obtained substituting the viscous yaw-dampers for friction dampers. All analyses have been performed with a conventional coefficient of friction equal to μ_k =0.15, while the normal load between the rubbing surfaces of the friction damper has been changed.

II.1 The ETR 460 and its model

The ETR 460 is a distributed power train composed of nine vehicles grouped into three traction units comprising two motor cars and one trailer. The electric traction equipment has a total power of 6000 kW (500 for each motor bogie). The cars also feature a tilting capability, devised in order to negotiate curves with higher values of non-compensated lateral acceleration on the bogie (up to 1.8 m/s^2) which produced to the train the commercial name of PENDOLINO.
The ADAMS/Rail model of the ETR 460-BAC used for the numerical simulations presented in this work is the result of a cooperation between Politecnico di Torino and Fiat Ferroviaria S.p.A. (Savigliano, Italy). This model is documented in previous works ([6] [7]) and articles ([8],[9],[10]).It consists of 31 rigid bodies, namely 1 car body, 2 bogies, 4 wheelsets, 8 axle boxes, 8 superior trusses, 8 inferior trusses. Primary and secondary suspensions are modeled using the ADAMS *FIELD* elements. The stiffness of the trusses is also taken into account. All dampers (vertical, lateral and yaw dampers) are modeled as the series of a linear spring and a nonlinear damper.

II.2 <u>Stability on Tangent Track using transient analysis</u>

The stability of the vehicle with respect to the hunting motion is estimated on a rigid tangent track without irregularities and using the linearized contact level of ADAMS/Rail (level IIa).
In the case of high grade of non-linearity due to the friction dampers the *critical speed*, limiting the threshold of instability of the vehicle, is found trough iterative transient analyses. (*as the critical speed of this vehicle is not public, speeds reported in the following figures are divided by a conventional number* V_o)
A lateral impulsive force has been applied on the center of mass of the front wheelset of the front bogie in order to excite the hunting motion. The lateral impulse is modeled as a piece-wise third order polynomial (STEP functions of ADAMS). A time duration of 0.05 seconds has been found to be small enough for obtaining the wanted accuracy on the critical speed estimation.
If the lateral force is applied, the critical speed tends to reduce, until a limiting value. obtained for a force magnitude equal to 10 kN. In *Figure 6* and *Figure 7* for different values of conicity (0.18, 0.28) is shown the same optimal value of force magnitude equal to 10 kN.
For the ETR 460-BAC, it is found that if no lateral force is applied the critical speed obtained through linearized analyses is very close to that obtained from transient analyses,

the differences being smaller for lower conicity values (Figure 8). This is essentially due to the fact that for low conicity the viscous antiyaw damper works in the linear part of the characteristic.

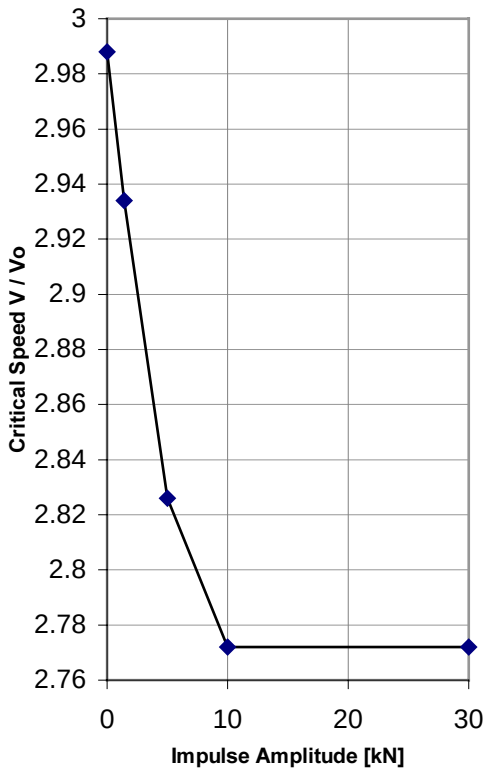

Figure 6: Critical speed vs. impulse magnitude ETR 460-BAC conicity=0.18

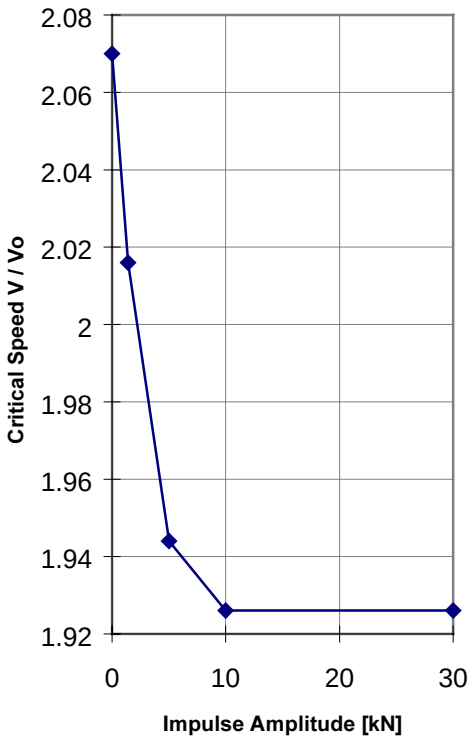

Figure 7: Critical speed vs. impulse magnitude. ETR 460-BAC Conicity=0.28

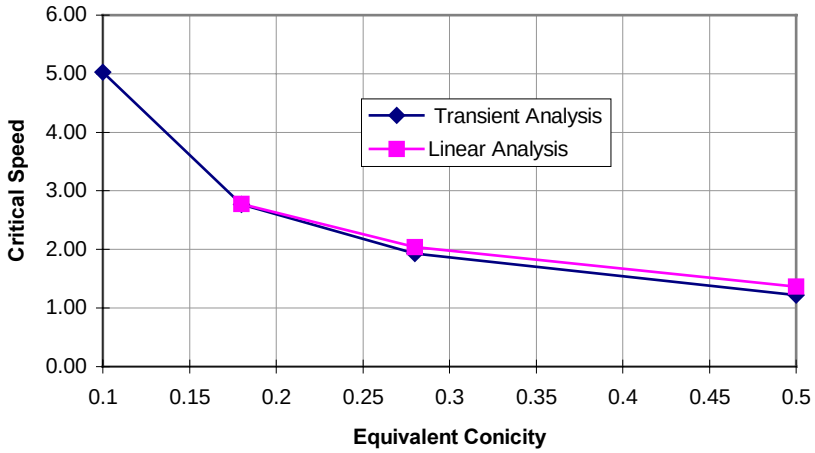

Figure 8: Effect of equivalent conicity on critical speed

Different patterns have been obtained when considering the friction damped vehicle. The steepness of the friction-velocity curve about the origin locks-up the yaw rotation of the

bogie and therefore the hunting motion is limited to wheelsets and is not transmitted to the bogies, unless disturbances are applied. As a result linear analyses and transient analyses run in absence of lateral disturbances led to critical speed 4 to 6 times greater than those coming from 10 kN-disturbance transient analyses reports the sensitivity of the ETR 460-FD to the lateral disturbance magnitude for conicity equal to γ=0.18 and γ=0.28.
The normal load (N_l) acting on the friction dampers has been taken such that the critical speed of the ETR 460-BAC the ETR 460-FD is the same for a lateral disturbance of 10 kN and an equivalent conicity γ=0.18 with a friction coefficient μ_k =0.15. This value was found to be equal to N_l =11.34 kN.
However if the lateral disturbance is increased the critical speed of the friction damped vehicle is noticeably diminished. In particular increasing the impulse magnitude from 10 to 30 kN the critical speed is reduced by 48% and 43% respectively for the two values of conicity considered.

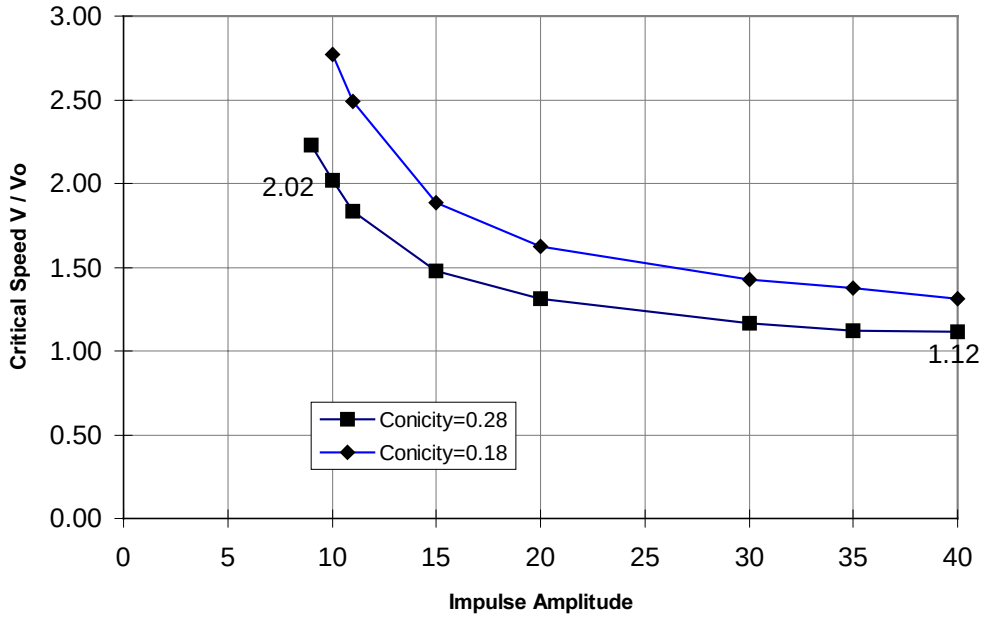

Figure 9: Critical speed vs. impulse magnitude (ETR 460-FD N_load=12 kN)

A first result (comparing Figure 6 and Figure 7 with Figure 9) is the different sensitivity to lateral impulses magnitude. The ETR 460-FD is far more sensitive to impulse magnitude variation.
On the other hand friction dampers have been observed to provide an excellent efficiency in extinguishing oscillations for undercritical speeds Figure 11**.** For a speed 1% below the critical value oscillations are damped out in about seconds using friction devices, while viscous yaw-dampers require always more than 10 seconds to reduce noticeably (but not to damp out) oscillations (Figure 10).

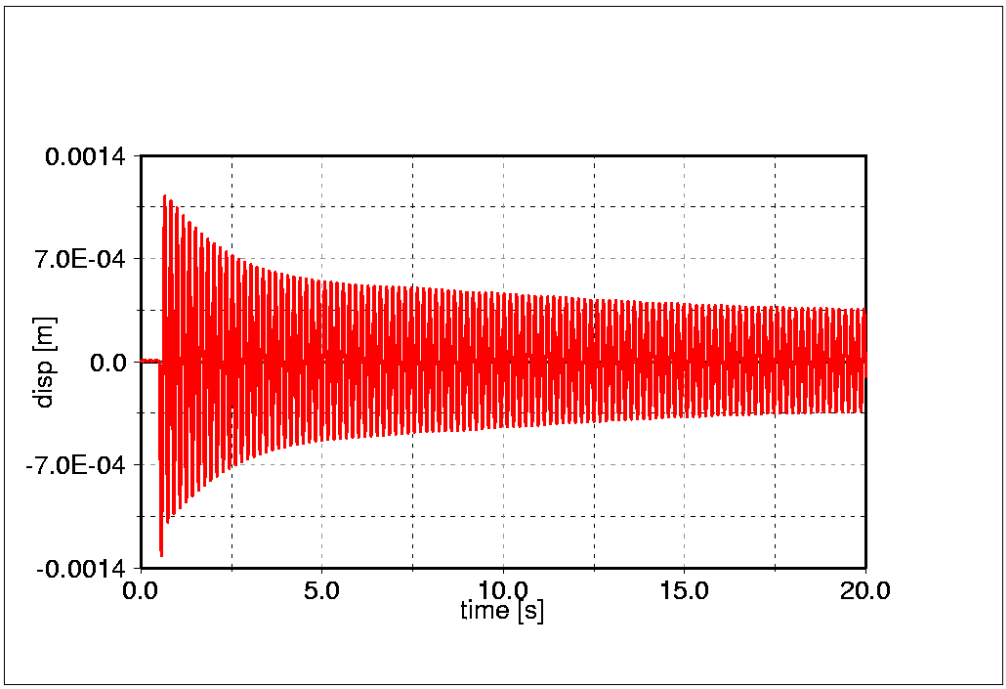

Figure 10: Oscillation of Wheelset1 at 1% below critical speed. (ETR 460-BAC)

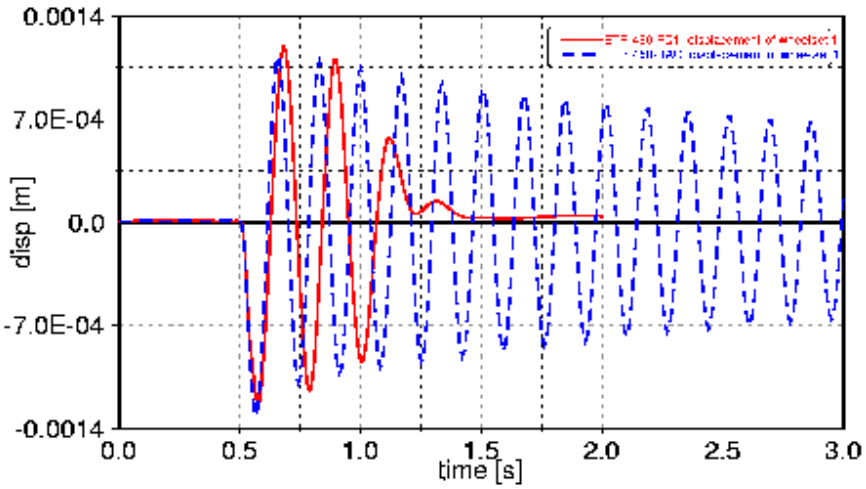

Figure 11: Oscillation of wheelset 1 at 1% below critical speed. Red: ETR 460-FD Blue: ETR 460-BAC

At any rate the growth of the normal load between the sliding surfaces of the friction damper leads to an increase in the critical speed of the ETR 460-FD (e.g. see figure 12).

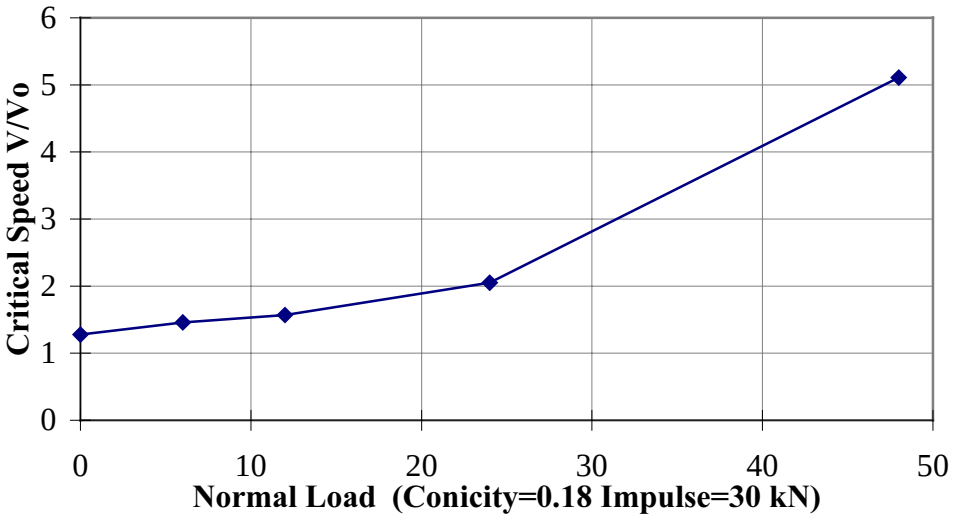

Figure 12: Critical peed vs. normal load (ETR 460-FD)

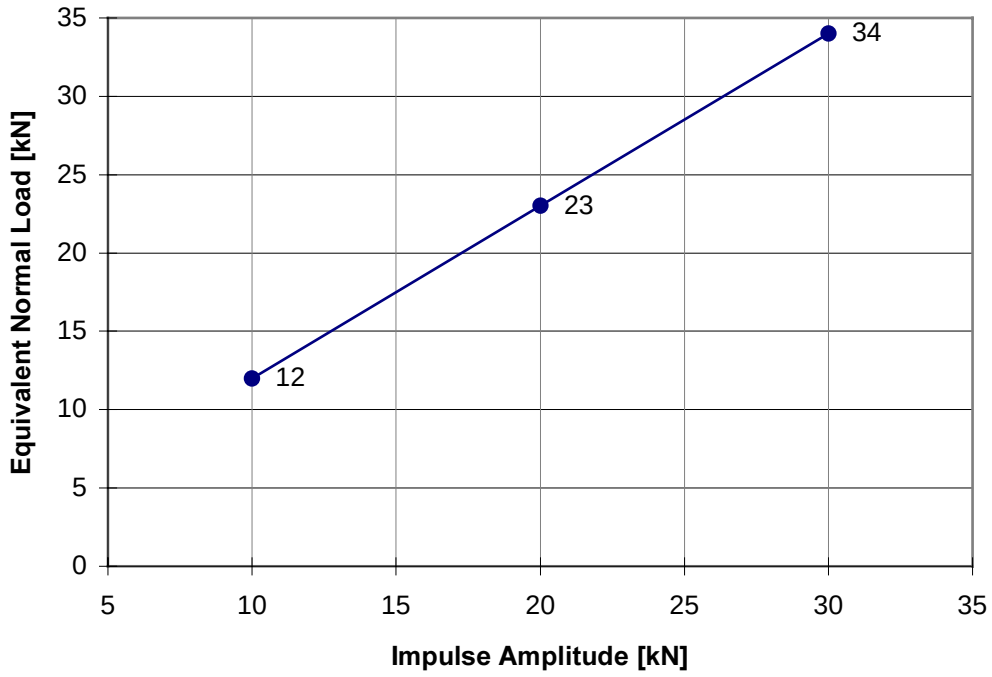

Fig 13 Equivalent normal load vs. impulse magnitude (conicity=0.18)

As a consequence, for any value of the lateral disturbance and equivalent conicity a value of the normal load can be found allowing the same critical speed of the ETR 460-BAC . This value has been defined *equivalent normal load*.
In figure 13 the equivalent normal loads for lateral inputs ranging from 10 to 30 kN are represented. Figure 14 reports the sensitivity of the equivalent normal load with respect to the variation of equivalent conicity. It is noted that for impulses of 10 kN the highest value found is 12 kN. A reduction of 12% is noted if the conicity passes from 0.10 to 0.28.

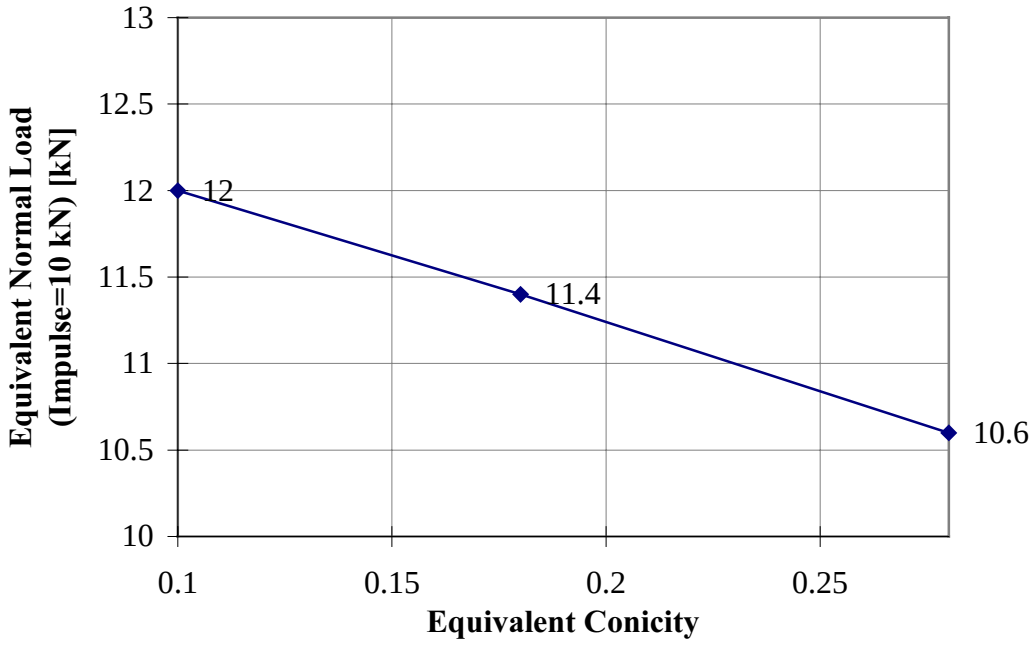

Fig 14 Equivalent normal load vs. equivalent conicity

In figure 15 the sensitivity with respect to the static to kinetic friction coefficient is reported. The values chosen for the other variables are:

VD = 7 10^{-3} m/s	AC= 5 10^{-3} m/s^2	VK=10^{-3} m/s
VM=3 10^{-3} m/s	Impulse = 10 kN	Conicity=0.18

Normal Load = 11340=$Nl_{eq,c=0.18,Fo=10}$

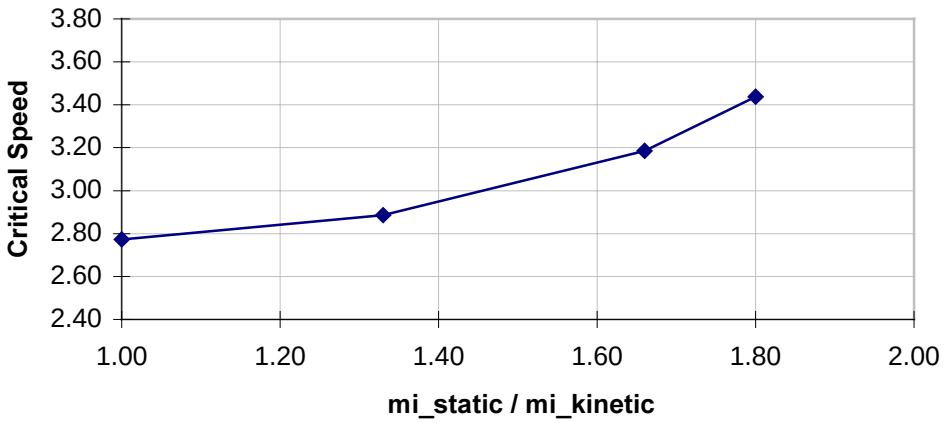

Figure 15 Effect of the static coefficient of friction on critical speed

II.3 Curve Negotiability

Curves negotiation requires a yaw rotation of the wheelsets with respect to the bogies and

of the bogies with respect to the car body.
As a consequence there is a trade-off between a high rotational rigidity of primary and secondary suspensions to control hunting stability and a high flexibility of them to facilitate curve negotiation. Similar considerations can be done for the yaw dampers, as the curve entry and curve exit requires certain relative a rotation velocity.
The use of friction yaw-dampers may lead to further difficulties as the maximum friction force is exerted for small relative rotation velocity. When the relative rotations become insufficient some wheel may climb the rail and derailment occurs.
The possibility of a wheel climb is measured in terms of the maximum lateral forces or lateral to vertical force ratios (Y-Q ratio) exerted on the outer wheel of the front wheelset. The maximum relative angle between the front wheelset and the local curve radius, the attack angle, is also taken into account.
In this section the results of simulation of curve entry are presented for the ETR 460-FD1 in comparison to ETR 460-BAC. The track has a 500 meters radius and a maximum superelevation of d=0.16 meters. It is preceded by a 50 meters spur track having curvature and superelevation linearly variable from zero to the maximum value. The gauge (2s) is constant and equal to the nominal value of 2s=1.435 meters. No flexibility has been allowed to the track or to the wheelsets.
Various tangential speeds have been attempted, however the maximum wheel to rail interactions have been found for the highest values.
In the following figures the maximum lateral force (figure 16) and lateral to vertical force ratio (figure 17) for the outer wheel of the first wheelset and the maximum attack angle of the first wheelset (figure 18) recorded are reported for the ETR 460-FD for various values of the normal load acting on the sliding surfaces of the dampers (the kinetic coefficient of friction is still 0.15). The horizontal axis of the diagrams has been put in correspondence to the values obtained for the ETR 460-BAC. In all cases the tangential speed of the train (v) is equal to 37.73 m/s corresponding trough formula (II.1) to a non-compensated acceleration (nca) of 1.8 m/s^2.

$$nca = \frac{v^2}{R} - \frac{g \cdot d}{2 \cdot s} \qquad \text{(II.1)}$$

v =tangential speed of the vehicle 37.725 m/s
d =track superelevation= 0.16 m
2s =gage=1.435 m
R =curve radius=500 m
g =acceleration of gravity=9.81 m/s^2

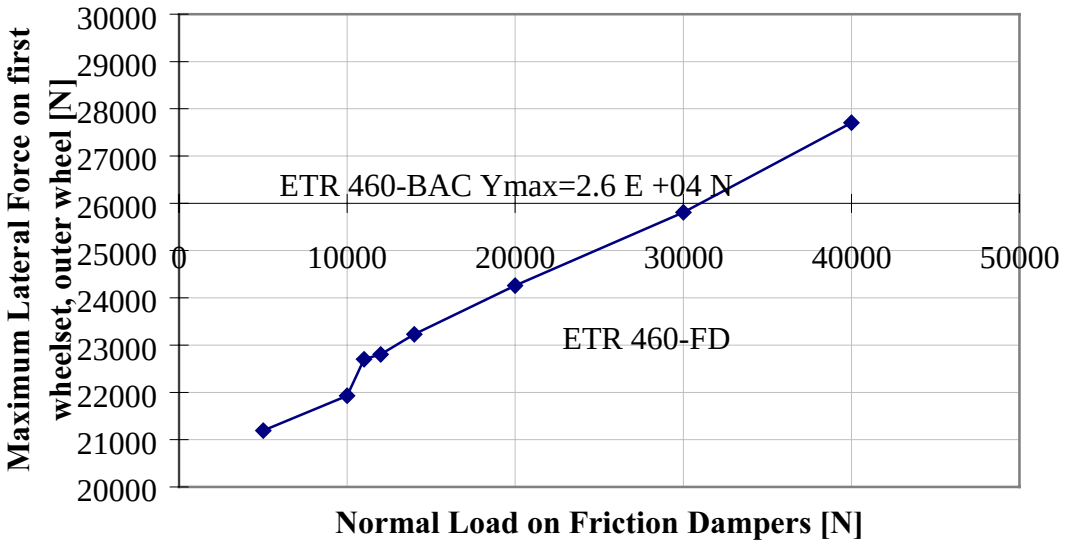

Figure 16 Maximum lateral force (Y max) on the outer wheel of the front wheelset for the ETR 460-FD in comparison to the ETR 460 BAC

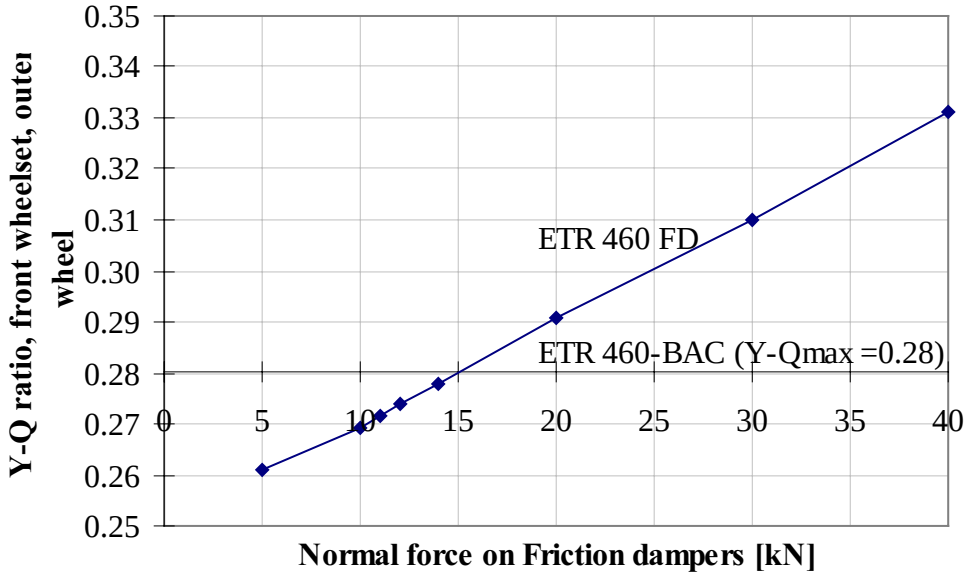

Figure 17 Maximum lateral to vertical force ratio (Y-Q max) on the outer wheel of the front wheelset for the ETR 460-FD in comparison to the ETR 460 BAC

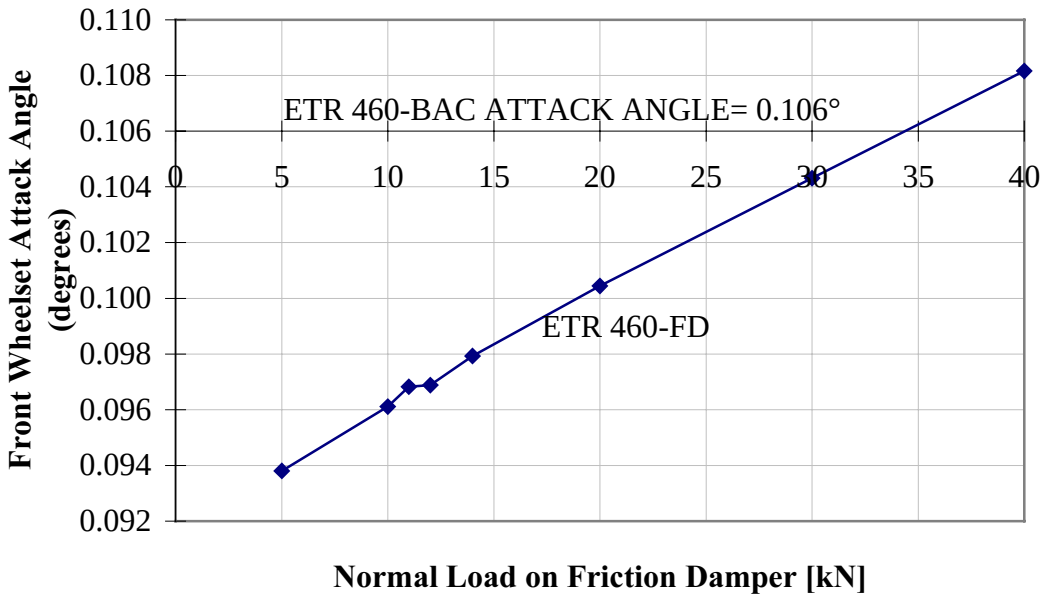

Figure 18 Maximum attack angle of the front wheelset for the ETR 460-FD in comparison to the ETR 460 BAC

From the above figures the following considerations may be drawn:

- The increase of normal load on the friction dampers, preventing the bogies from rotating freely in curve entry, always reduces curve negotiation capability.
- Only for normal loads smaller than 15 kN it can be assumed that the ETR 460-FD performs better curve entry than the ETR 460-BAC. For this load, however the vehicle would be stable only against lateral disturbances of the order of 13 kN or smaller (13 kN has been obtained interpolating linearly from the figure 7). If stability is to be achieved against lateral wheelset pulses of the order of 30 kN, the maximum expected to occur without the track safety be seriously diminished, normal loads of the order of 34 kN are necessary (assuming friction coefficient equal to 0.15).
- In this case when entering the curve both the lateral pulses on the outer front wheel and the attack angle are very close to the values obtained for the ETR 460-BAC (differences being of the same order of results accuracy: 2%), while the maximum Y-Q ratio of the ETR 460-FD is about 15% higher than that of the ETR 460-BAC (0.32 against 0.28), but always laying largely below values considered critical

III. Conclusions

Friction dampers are proved to be very effective in railway applications as they are able to reduce hunting oscillations much more quickly than conventional viscous dampers. They also lead to some structural advantages as the global force sustained by the dampers is reduced with respect to viscous dampers.

The ETR 460-FD performs much better than the ETR 460-BAC both on tangent and curved track if the dampers are set in order to allow the same critical speed of the ETR 460-BAC against maximum lateral wheelset pulses of the order of 13 kN. This case obviously excludes the switch crossing, but includes long straight tracks with medium irregularities. In switch crossing either a reduction of the critical speed or an increase of the normal load on the dampers is to be accepted, the latter choice leading to poorer curve negotiability. Global improvements to the performances of the ETR 460 can be achieved resorting to a controlled friction dampers with variable normal load Electronic control could be able to adjust the normal load on the dampers to the track characteristic.

Friction dampers can be used instead of viscous dampers for obtaining the same critical speed with higher Y-Q ratio but with very excellent and efficient damping. In addition the overall bogie weight can be reduced, as the tangential forces to be sustained is smaller.

References

[1] Rabinowicz E.: *Friction and Wear of Materials* (Wiley, New York, 1995)

[2] Wang, M., *Untersuchungen über hochfrequente Kontaktshwingungen zwischen rayen Oberflächen*, Doctoral Thesis, 1994, Technische Universität Berlin.

[3] Sakamoto, T., *Normal Displacement and Dynamic Friction Characteristics in a Stick-Slip Process*, Tribology International, Vol 20 (1987), pp. 25-31

[4] Cockerham,G., and Cole, M., *Stick-Slip Stability by analogue Simulation*, Wear, Vol 36(1976), pp.189-198

[5] Sampson, J.B., Morgan, F., reed,D.,W., and Muskat, M., *Studies in Lubrication XII: Friction Behavior during the Slip Portion of the Stick-Slip rocess*, J.Appl. Phys., Vol.14 (1943), pp.689-700

[6] Bo,L.,C., and Pavlescu D., *The Friction-speed relation and its influence on the critical velocity of Stick-Slip Motion*, Wear, Vol.82 (1982), pp.277-289.

[7] McMillan, A.,J., *A Non-Linear Friction Model for Self-Excited Vibrations*, Journal of Sound and Vibrations, Vol.205 (1997), pp.323-335.

[8] Bogo,C., *Analisi Numerica Della Stabilità Laterale di un Veicolo Ferroviario ad Alta Velocità*, Thesis, Politecnico di Torino - Seconda Facoltà di Ingegneria, 1997

[9] Gugliotta, A., Somà, A., Arrus,P., *Modeling the dynamic behavior of a yaw damper and its implementation in ADAMS/Rail*, Adams/Rail User-Meeting, Utrecht 28-29 April 1997

[10]Gugliotta,A., Somà,A., Arrus,P., *Studio della Stabilità Laterale di un Veicolo Ferroviario*, AIAS'97, Catania 3-5 september 1997

[11] Vivalda,P., Giuizio,R., Gugliotta,A., Somà,A., Arrus,P., *Stability Analysis of High Speed Train with Adams/Rail Numerical Simulation* , Computer simulation of rail vehicle dynamics, Manchester, Giugno 1997.